

# Recursion equations in predicting band width under gradient elution

Heng Liang\*, Ying Liu

*The Key Laboratory of Biomedical Information Engineering of Education Ministry, Separation Science Institute,  
Xi'an Jiaotong University, Xi'an 710049, People's Republic of China*

Received 4 November 2003; received in revised form 17 March 2004; accepted 23 March 2004

## Abstract

The evolution of solute zone under gradient elution is a typical problem of non-linear continuity equation since the local diffusion coefficient and local migration velocity of the mass cells of solute zones are the functions of position and time due to space- and time-variable mobile phase composition. In this paper, based on the mesoscopic approaches (Lagrangian description, the continuity theory and the local equilibrium assumption), the evolution of solute zones in space- and time-dependent fields is described by the iterative addition of local probability density of the mass cells of solute zones. Furthermore, on macroscopic levels, the recursion equations have been proposed to simulate zone migration and spreading in reversed-phase high-performance liquid chromatography (RP-HPLC) through directly relating local retention factor and local diffusion coefficient to local mobile phase concentration. This new approach differs entirely from the traditional theories on plate concept with Eulerian description, since band width recursion equation is actually the accumulation of local diffusion coefficients of solute zones to discrete-time slices. Recursion equations and literature equations were used in dealing with same experimental data in RP-HPLC, and the comparison results show that the recursion equations can accurately predict band width under gradient elution.

© 2004 Elsevier B.V. All rights reserved.

*Keywords:* Recursion equations; Solute migration; Band broadening; Band width prediction; Gradient elution

## 1. Introduction

Generally, solute zones synchronously undergo two movements with opposite-effects, relative migration and spreading in column separation processes [1,2]. Accurately predicting the migration and spreading of solute zone, especially, under gradient elution is the first task, though analysts are mostly interested in finding optimal parameters with satisfactory separation efficiency.

Chemometric approaches and function models are always used in predicting zone migration. Sun et al. adopted a mixture design simplex method for computer-assisted optimization of the mobile phase composition [3], and Vivo-Truyols et al. simulated peak with an asymmetrical peak model [4]. Lisseter optimized ternary mobile phases with a seven-point factorial design [5]. Vanbel used a sigmoidal model to describe capacity factors, peak heights and peak areas [6]. The advantage of chemometric tools is that no explicit models

are required, conversely, it requires a relatively a larger number of experiments to perform to make it applicable.

When the models with physical chemistry meanings are available, chromatographic optimization is easier to perform with regression methods. Some regression parameters can be obtained with chromatographic model and limited number of experiments. Then optimal separation conditions can be found through a computer-assisted optimization with the model and regression parameters. Snyder and co-workers developed the linear solvent strength (LSS) model [7,8] widely applied in retention prediction. Schoenmakers et al. [9,10] derived the solubility parameter model and the inter-phase model using solubility parameters. Geng and Regnier [11,12] proposed the stoichiometric displacement model (SDM), a logarithmic dependence of retention to modifier concentration. Jandera and others widely studied gradient elution [13,14], and derived two important equations on the retention models of the retention volume in reversed-phase high-performance liquid chromatography (RP-HPLC), normal-phase or ion-exchange. These retention models can fit some retention data very well.

\* Corresponding author. Tel./fax: +86-29-82663992.

E-mail address: [lheng@mail.xjtu.edu.cn](mailto:lheng@mail.xjtu.edu.cn) (H. Liang).

For band dispersion, Martin and Synge [15] originally proposed the concept of “height equivalent to one the theoretical plate”, which is defined as the thickness of the layer such that the solution issuing from it is in equilibrium with the mean concentration of solute in stationary phase throughout the layer. The definition indicated that the whole separation path is assumed to be divided into a series of linked stages or plates, and the mean solute concentrations in the mobile or stationary phase in a layer (or a plate) change continuously with serial number of plate and time coordinate. The assumptions were made that the distribution ratio of one solute between the two phases at equilibrium in one plate. The early Craig plate model used a great number of identical separation flasks connected in series to simulate chromatographic column [17]. van Deemter et al. [16] related plate height to the flow velocity of mobile phase, which was widely applied in multiform column separations. Horavth [18], Poppe et al. [19] and other scientists made important contributions to the field.

The continuity equation describing the migration and shape of solute zones is used to construct plate theory [1,2,20]. Giddings defined plate height as the ratio of the total effective diffusion coefficient ( $D$ ) to uniform translation velocity ( $v$ ) of solute zones in the whole process of column separation [1]. In fluid mechanics, there are two basic description method, Lagrangian method and Eulerian method. Lagrangian description method is to keep track of identifiable elements of mass (e.g. in particle mechanics), and Eulerian description method focuses attention on the properties of a flow at a given point in space as a function of time, in which the properties of a flow field are described as functions of space coordinates and time [21]. In fact, Plate theory only adopted a utilitarian method which appears like Eulerian description due to that plate height is a constant for given chromatographic system, but could not be as cells (or layers) small enough so that the thermodynamic properties of the system vary little over each cell.

The literature concerning gradient elution showed that there were unacceptable errors in the theoretical calculation of band widths with theoretical plate, and sometimes the error can reach 50% [7,13] although the agreement between experiment and theory was satisfactory for the prediction of retention volumes. In fact, the unacceptable calculation errors of band widths are unavoidable as long as one adopts the concept of plate height, because the composition of the mobile phase affects local plate height in separation processes through space- and time-variable axial dispersion coefficient and axial migration velocity. To get over this limitation, Giddings introduced the concept of the local plate height, but he and the other scientists did not do further detailed researches on this subject [1]. Therefore, we need an original theoretical model to gain some breakthrough in the framework of plate theory [22–24], and to describe solute retentions and band dispersions synchronously and more truly, which is a base to obtain optimal gradient profiles for given solute and separation system with the methods of modern cybernetics un-

der gradient elution or other similar cases. Non-equilibrium thermodynamic separation theory in preceding papers could be used to establish the recursion equations [20,22–28].

In this paper, we originally present two recursion equations concerning the migration and spreading of a cell occupied by the solute with a fixed, identifiable quantity of mass or probability (Lagrangian description), which observably differ from the methods of plate theory (Eulerian description). The validity of recursion equations is examined by the examples of reversed-phase under isocratic and gradient elution of small molecular series. The results show that recursion equations have more advantages in predicting band widths than the literature equation [14].

## 2. Theoretical

### 2.1. The summarization of non-equilibrium thermodynamic separation theory (NTST)

It is considered that NTST separation processes are certainly irreversible due to the fact that solute zones non-homogeneously and space–time varyingly distribute in space- and time-dependent fields, and the solute in each small volume cell that solutes occupied jointly are open systems of thermodynamics in applied fields (e.g. electric field and chemical potential, etc.) [2,23–25]. Clausius’ heat death (band spreading of one component) and Darwin’s evolutionism (separating among different components) simultaneously coexist in separation processes [2]. The two opposite processes originate simultaneously from the irreversibility of separation processes, which are described quantitatively by the items of entropy production and entropy flows, respectively. The entropy balance equation in non-equilibrium thermodynamics has been used to reveal quantificationally the irreversibility of separation processes, which is the framework of NTST instead of the framework of contemporary separation theories based on the mass conservation equation with dynamic methods. With recursion equations and multi-objective cost function (including integral optimizing functional, separation time, the length of separation path and solute band width), we could find the optimal thermodynamic separation path or optimal decision sequence through using non-equilibrium thermodynamic separation theory, multi-stage decision and optimal control methods [25–28].

### 2.2. Discrete space–time of solute zones

In separation processes, the diffusion and migration as two essential physical chemistry phenomena belong to the category of linear non-equilibrium thermodynamics [29,30]. The assumption of the local equilibrium in non-equilibrium thermodynamics was described as “it must be assumed that the mass or volume elements (cells) of a continuous medium can be considered as equilibrium state parameters despite

the fact that various processes take place between the neighbouring cells. As a consequence of this condition—which is usually called local equilibrium” [29]. The local equilibrium assumption as a foundation stone in non-equilibrium thermodynamics [30] allows us to divide the topological space occupied by solutes (at given time) into cells small enough so that the thermodynamic properties of the system vary little over each cell but large enough so that the cells can be treated as macroscopic thermodynamic subsystems in contact with their surroundings. The assumption also allows us to divide the overall evolution time of a complex system into many small time intervals. Thus the assumption ensures that we can structure discrete space–time systems in order to control the separation systems time-varyingly [31,32].

On the viewpoint of mechanics of continuous media [33,34], the spreading and the relative migration of solute zones as two basic macro motions on the separation path ought to belong to the ‘deformation’ and ‘flow’ motions of continuous media, respectively. To catch hold of the basic characters of the both macro motions of solute zones, we could consider that the infinite small volume elements,  $d\Omega = A dx$ , of the solute zone (the component  $i$ ) stretches with the ‘stretch ratio’  $\lambda_{i,k}$  along separation path. It is clear that the stretch motion of volume elements only occurs in the fluid of same component. This stretch motion corresponds to the diffusion motion that leads to the configuration change of the solute zone distribution. Synchronously, the volume element marked  $j$  in the solute zone slip with a time-varying velocity,  $\vec{v}_{i,j,k}$ , at the time  $t_k$ , which must differ from other component’s along separation path. The motions of solute zones are shown visually in Fig. 1 on Lagrangian description and local equilibrium assumption in fluid dynamics.

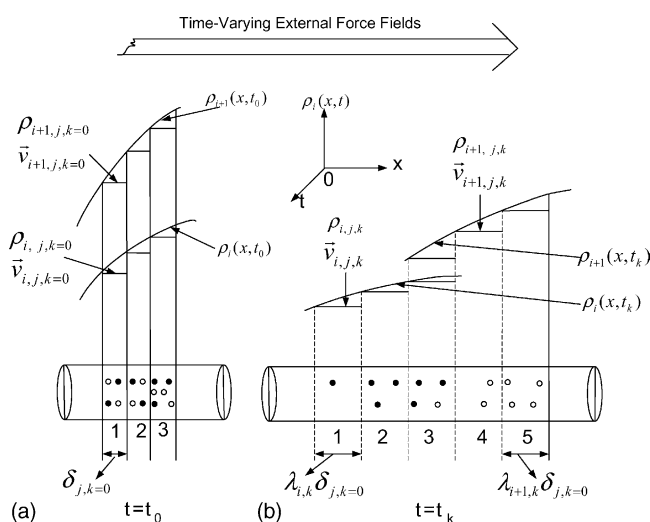


Fig. 1. The two motions of infinitesimal volume elements of solute zones are in both typical motion forms, ‘deformation’ (spreading) and ‘flow’ (relative migration) in time-varying external force fields at the time interval between  $t = t_0$  (a) and  $t = t_k$  (b).

In Fig. 1, we arbitrarily chose three adjoining volume elements of the two components,  $i$  and  $i + 1$ , which are in the region  $x_0 \sim x_0 + \delta_{j,k=0}$  ( $j = 1, 2, 3, \dots, J$ ), where  $\delta_{j,k=0}$  is the length of the volume element  $j$  on  $x$  axis along separation path at initial time  $t_{k=0}$  in Fig. 1a. The local solute densities of two components,  $i$  and  $i + 1$ , are  $\rho_{i,j,k=0}$  and  $\rho_{i+1,j,k=0}$  in the region. Apparently, these local solute densities determine corresponded macro density distributions,  $\rho_i(x, t_0)$  and  $\rho_{i+1}(x, t_0)$ , of solute zones. Local velocities of the volume elements of the components  $i$  and  $i + 1$  can be indexed by time-varying velocities,  $\vec{v}_{i,j,k}$  and  $\vec{v}_{i+1,j,k}$  due to that the volume elements are in time-varying external fields. For any effective separation process, there is the relationship,  $\vec{v}_{i,j,k} \neq \vec{v}_{i+1,j,k}$ , which just causes the slip motion between the volume elements of two separable components. Along the direction of ‘the arrow of time’ [35] ( $t_k < t_{k+1}$ ), the solute system will evolve a new state that the volume elements would have a new local solute densities in Fig. 1b., where  $\rho_{i,j,k}$  in the region  $x_k \sim x_k + \lambda_{i,k}\delta_{j,k=0}$  and  $\rho_{i+1,j,k}$  in  $x_k \sim x_k + \lambda_{i+1,k}\delta_{j,k=0}$  with local velocities  $\vec{v}_{i,j,k}$  and  $\vec{v}_{i+1,j,k}$ , respectively.

There are two accepted and essential assumptions in column separations: (1) the total amount of one solute is constant in separation processes; (2) one type of distribution curve can describe one solute distribution at any separation time, such as Gaussian distribution or one kind of exponentially modified Gaussian distributions [36,37]. The two assumptions can be traced to fluids’ deformation motion in fluid dynamics with the axiom of continuity—any deformation can only be described by single valued transformations which can be continuously differentiated as many times as required [33,34]. Based on the description of the mesoscopic approach [38], we can consider that a separation process is a set of the combination of solutes’ volume elements that simply stretch and move on separation path in external force fields.

In separation science, space- and time-dependent fields,  $u_{j,k}$ , generally include the chemical potential between mobile and stationary phase due to the space- and time-dependent solvent strength under gradient elution [13,2], or due to the space- and time-dependent solute concentration in non-linear chromatography [39], or due to time-varying electric field in capillary electrophoresis [40], etc. With the local equilibrium assumption we can define a set of local thermodynamic variables in given volume element  $j$  of solute zone  $i$  at the time  $t_k$  in separation processes, such as local molar concentration,  $c_{i,j,k}$ , local migration velocity,  $\vec{v}_{i,j,k}$ , local diffusion coefficient,  $D_{i,j,k}$ , local thermodynamic distribution constant,  $K_{i,j,k}$ , and local capacity factor,  $k'_{i,j,k}$ , etc. Accordingly, we can define local external force fields that acts on the given volume element  $j$  of the solute zone  $i$  at the time  $t_k$ , these local external force fields include local strong eluent concentration of mobile phase,  $\varphi_{i,j,k}$ , local chemical potential,  $\mu_{i,j,k}$ , and electrical field strength,  $E_{i,j,k}$ , etc. One can use any thermodynamic laws with local thermodynamic variables in the identifiable volume elements [29,30].

### 2.3. General recursion equations in column separation

In the time interval  $\Delta t_{i,k}$ , the migration distance of the volume element  $j$  of the solute zone  $i$  along the longitudinal direction ( $x$  coordinates) in stationary phase is  $\Delta X_{i,j,k} = X_{i,j,k+1} - X_{i,j,k}$  with the local migration velocity,  $\bar{v}_{i,j,k}$ , in space- and time-dependent fields, where  $X_{i,j,k}$  and  $X_{i,j,k+1}$  are the migration positions of the volume element  $j$  in stationary phase at the time  $t_k$  and  $t_{k+1}$ , respectively. So the recursion equation concerning migration position of the cell  $j$  can be expressed as:

$$X_{i,j,k+1} = X_{i,j,k} + \bar{v}_{i,j,k} \Delta t_k \quad (1)$$

Eq. (1) indicates the slip motion of the cell  $j$  of the solute  $i$ , and means that the migration distance of the solute is the accumulation of the local migration velocity to the migration time. In linear non-ideal chromatography it does not need to distinguish the number of the volume element,  $j$ , due to the same thermodynamic behaviours of each volume element. In this case, we can predigest the local variables, such as from  $\bar{v}_{i,j,k}$  to  $\bar{v}_{i,k}$ , or from  $\varphi_{i,j,k}$  to  $\varphi_{i,k}$  or  $X_{i,j,k+1}$  to  $X_{i,k}$ , etc. The initial condition of Eq. (1) is  $X_{i,0} = 0$  when the solute is at the column inlet at the run beginning. Its termination condition is  $X_{i,K} = L$ , when the solute is at the column terminal at the end of separation process,  $t_K = t_R$ , where  $t_R$  is solute retention time. We call Eq. (1) general migration recursion equation of solute zones.

We may choose  $[-2\sigma, 2\sigma]$  as the research region of a solute zone, of course,  $[-3\sigma, 3\sigma]$  or bigger research regions can also be chosen, where  $\sigma$  is standard deviation of solute zone distribution. Based on the local equilibrium assumption and the axiom of continuum (Fig. 1) we can obtain the recursion equation concerning the stretch of a cell in  $\Delta t_k$ ,

$$m_{i,j,k+1} = \sqrt{m_{i,j,k}^2 + \left(\frac{32}{J^2}\right) D_{i,j,k} \Delta t_k} + (\bar{v}_{i,j+1,k} - \bar{v}_{i,j,k}) \Delta t_k \quad (2)$$

where  $m_{i,j,k+1}$  and  $m_{i,j,k}$  are the volume element width along column axes of the cell  $j$  of solute  $i$  at the time  $t_{k+1}$ , at the time  $t_k$ , respectively. And  $\bar{v}_{i,j+1,k}$  is the linear velocity of the cell  $j+1$  of the solute  $i$  in  $\Delta t_k$  along  $x$  coordinates. The first term at the right-hand side of Eq. (2) is the local diffusion term of the cell  $j$ , which means the accumulation of the local apparent diffusion coefficient to the migration time, and the increment of this term is always positive since  $D_{i,j,k} > 0$ . And the second term at the right-hand side of Eq. (2) is the contribution to the width of the cell due to the overlapping and stretching between adjacent cells, and this term may be negative, zero and positive, which brings the distortion of band shape. This term will play an important role in non-linear chromatography, although it is not discussed in this paper. We call Eq. (2) general diffusion recursion equation of the cells of the solute zone.

In linear non-ideal chromatography, the second term at the right-hand side of Eq. (2) is zero due to  $\bar{v}_{i,j+1,k} = \bar{v}_{i,j,k}$ . Therefore, Eq. (2) can be predigested as:

$$\sigma_{i,k+1}^2 = \sigma_{i,k}^2 + 2D_{i,k} \Delta t_k \quad (3)$$

where  $\sigma_{i,k}$  and  $\sigma_{i,k+1}$  are the solute standard deviation at the times  $t_k$  and  $t_{k+1}$ , respectively. The initial condition of Eq. (3) is the solute standard deviation at the beginning of separation,  $\sigma_{k=0} = (\sqrt{3}/6)(V_0L)(Ft_0)$ , and  $V_0$  is the injected solute column,  $L$  the column length,  $F$  the volume flow-rate of mobile phase,  $t_0$  the column dead time. The termination condition of Eq. (3) is the solute standard deviation at the end of separation process when  $t_{K,i} = t_{R,i}$ . Eq. (3) indicates that the incremental part of the standard deviation  $\sigma_{i,k}$  (corresponding to the solute band width) of the solute zone  $i$  arises from the accumulation of  $D_{i,k}$  to  $\Delta t_k$ .

### 2.4. Band width recursion equation in RP-HPLC

In gradient elution solute zones are acted at any time in the space- and time-dependent field due to the space- and time-dependent solvent strength [8,13], which can be expressed by local strong eluent concentration of mobile phase,  $\varphi_{i,j,k}$ . And the local chemistry potential  $\mu_{i,j,k}$  or local capacity factor  $k'_{i,j,k}$  is determined by the local mobile phase composition,  $\varphi_{i,j,k}$ , which veritably affects the migration and broadening of the cell  $j$  of the solute  $i$  at  $t_k$ . For any gradient profiles of the strong eluent concentration in a multi-component mobile phase,  $\varphi = f(t)$ , it can be treated with infinite small segments of step gradient in the equal time unit,  $\Delta T_k$  (e.g. 0.1 min, whose magnitude is independent of the time serial number,  $k$ ). Thus, the gradient profiles of the strong eluent at the pump head can be described as concentration sequence  $\{\varphi_k\}$ . The well known integral equation of gradient retention [13] is:

$$\int_0^{t_R-t_0} \frac{dt}{t_0 k'(t)} = 1 \quad (4)$$

Considering the initial condition of the solute migration ( $X_{i,0} = 0$ ) and the termination boundary condition ( $X_{i,K} = L$ ), the discrete form of Eq. (4) can be written as:

$$\sum_{k=0}^{K-1} \left[ \frac{\Delta T_k}{t_0 k'_{i,k}} \right] = 1 \quad (5)$$

Through introducing the constant time unit  $\Delta T_k$  in Eq. (5), the boundary condition of the solute migration is expressed directly by the local capacity factor  $k'_{i,k}$ . The local equilibrium assumption in non-equilibrium thermodynamics allows that there is a local relation between  $k'_{i,k}$  and  $\varphi_k$ , which can be obtained from LSS model under isocratic elution in RP-HPLC [41],

$$\log k'_{i,k} = \log k_{w,i}^0 - s_i \varphi_k \quad (6)$$

where  $k_{w,i}^0$  and  $s_i$  are the experimental characteristic parameters for the given stationary, mobile phase and the solute,



and they are constant when  $\varphi_k$  changes in the certain range. With the known values of  $k_{w,i}^0$  and  $s_i$ , the local capacity factor sequence  $k'_{i,k}$  corresponding to  $\{\varphi_k\}$  can be obtained from Eq. (6). As long as  $\Delta T_k$  is prescribed and  $t_0$  is known, the sequence number  $K$  of the time unit corresponding to the time of the solute leaving the column can be confirmed with Eq. (5).

Based on the continuum principium in hydrodynamics, the time slice  $\Delta t_{i,k}$  (corresponding to the local capacity factor,  $k'_{i,j,k}$ ) during which the solute undergoes the certain  $\varphi_k$  in the column can be expressed by the time unit  $\Delta T_k$  during which the mobile phase keeps the same concentration  $\varphi_k$  at the outlet of the pump [42], the local relationship is obtained:

$$\Delta t_{i,k} = \frac{[(1 + k'_{i,k}) \Delta T_k]}{k'_{i,k}} \quad (7)$$

Considering the definition of local capacity factor,  $k'_{i,k} = (t_{R,k} - t_{0,k})/t_{0,k}$ , the iterative addition form of Eq. (4) is expressed:

$$t_{R,i} = \sum_{k=1}^{K-1} \Delta T_k + t_0 \quad (8)$$

where  $t_{R,i} = \sum_{k=1}^{K-1} \Delta t_{i,k}$  and  $t_0 = \sum_{k=1}^{K-1} t_{0,k}$ . Taking into account of the gradient dwell time,  $t_d$ , the retention time of the solute  $i$ ,  $t_{R,i}$  is:

$$t_{R,i} = \sum_{k=0}^{K-1} \Delta T_{i,k} + t_0 + t_d \quad (9)$$

Eq. (9) is a retention time equation with the iterative addition form, which directly corresponds to any gradient model,  $\{\varphi_k\}$  and  $\Delta T_k$ . It will be used to predict the solute retention time under gradient elution.

In isocratic elution there is an experimental linear relationship between half-band width ( $w_{1/2,t}$  in time units) and the instantaneous capacity factor,  $k'_f$ , when the peak maximum of the solute zone is just passing the end of the column [42]:

$$w_{1/2,t,i} = a_i + b_i k'_f \quad (10)$$

where  $a_i$  and  $b_i$  are experimental constants of the component  $i$  depending on the solute and on the chromatographic system. There is a basic relationship of the solute band broadening:

$$\sigma_{l,i}^2 = 2D_i t_{R,i} \quad (11)$$

where  $\sigma_{l,i}$  is the standard deviation of the zone distribution of the solute  $i$  in long measure. Considering three simple relationships as:

$$\begin{aligned} W_{1/2,l,i} &= \bar{v}_i W_{1/2,t,i}; & \bar{v}_i &= \frac{L}{t_0(1 + k'_f)}; \\ W_{1/2,l,i} &= 2.354\sigma_{l,i} \end{aligned} \quad (12)$$

Inserting Eqs. (10) and (12) into Eq. (11), we can obtain the local diffusion coefficient under isocratic elution:

$$D_i = \frac{0.09023L^2 (a_i + b_i k'_i)^2}{t_0^3 (1 + k'_i)^3} \quad (13)$$

Eq. (13) shows that the diffusion coefficient under isocratic elution is related to  $k'_i$ , experimental constants,  $a_i$ ,  $b_i$ , and system parameters.

Based on the continuum principium and the local equilibrium assumption, the local diffusion coefficient,  $D_{i,k}$ , under gradient elution can be obtained:

$$D_{i,k} = \frac{0.09023L^2 (a_i + b_i k'_{i,k})^2}{t_0^3 (1 + k'_{i,k})^3} \quad (14)$$

The cell  $j$  of the solute  $i$  passes the detector ( $X_{i,K} = L$ ) with the local migration velocity  $\bar{v}_{i,j,K-1}$  in the time interval,  $\Delta t_{K-1}$ , which needs a time interval, in the solute temporal distribution,  $\Delta \tau_{i,j}$ ,

$$\Delta \tau_{i,j} = \frac{m_{i,j,K-1}}{\bar{v}_{i,j,K-1}} \quad (15)$$

Eq. (15) will be used in the transforming of solute distributions from the spatial to the temporal one.

Considering Eqs. (3), (7), (14) and (15) and the solute band width arose by the dwell time,  $t_d$ , the half-band width with time unit,  $w_{1/2,t,i}$ , can be introduced by:

$$\begin{aligned} w_{1/2,t,i} &= 2.354 \sqrt{\frac{[\sigma_0^2 + \sigma_d^2 + \sum_{k=0}^{K-1} [2D_{i,k} \Delta T_k (1 + k'_{i,k})/k'_{i,k}]]}{\bar{v}_{i,K-1}^2}} \end{aligned} \quad (16)$$

where  $\sigma_d^2 = 2D_{i,k=0}t_d$ , and  $D_{i,k=0}$  the local diffusion coefficient of the solute  $i$  in the mobile phase composition  $\varphi_{k=0}$ . The gradient dwell time  $t_d$  is 0.0044 min for this HPLC instrument in the paper, and  $\sigma_d$  in Eq. (16) can be neglected nowadays for general HPLC instrument. The parameter  $\bar{v}_{i,K-1}$  is the local migration velocity of the solute zone along  $x$  coordinates in stationary phase in the last time interval,  $\Delta t_{K-1}$ . Eqs. (6) and (14) show that the parameters  $k'_{i,k}$  and  $D_{i,k}$  directly relate to  $\varphi_k$ , respectively, so  $w_{1/2,t,i}$  relates to  $\{\varphi_k\}$  through the two coefficients,  $k'_{i,k}$  and  $D_{i,k}$ . It implies that different  $\{\varphi_k\}$  induces different  $w_{1/2,t,i}$ . Eqs. (14) and (16) will be used to predict  $w_{1/2,t,i}$  corresponding to  $\{\varphi_k\}$  by inserting Eq. (14) into Eq. (16). For isocratic elution, Eq. (16) is also available by deleting the  $\sigma_d^2$  term. Eq. (16) is the band width equation of iterative addition form corresponding to  $\{\varphi_k\}$  in RP-HPLC.

### 3. Regression and prediction

For given solutes and column system the zone migration and broadening in gradient and isocratic elution can be predicted by using a computer program with Eqs. (5), (9), (14) and (16), respectively. In certain range the experimental constants,  $k_{w,i}^0$ ,  $s_i$ ,  $a_i$  and  $b_i$ , in Eqs. (6) and (10) only relate to

the varieties of modifier, solute and column system, but do not relate to  $\{\varphi_k\}$ . One must acquire these experimental constants at first through regression method with a limit number of experiments before the prediction of migration and broadening. In predicting zone migrations, the coefficients  $k_{w,i}^0$  and  $s_i$  are acquired with Eqs. (5), (6) and (9) by using non-linear regression [43]. Isocratic or gradient elution retention data acquired in a few preliminary runs (at least two runs) with different  $\{\varphi_k\}$  are employed to determine these experimental constants, and a non-linear least-squares curve-fitting program was used to obtain the best fit [43]. It is as a criterion that the estimated coefficients should minimize the sum of squares of absolute error between calculated retention time,  $t_{R,i,c}$ , and experimental retention time,  $t_{R,i,e}$ , of those preliminary runs, namely:

$$Q_{i,R} = \sum_{j=1}^n (t_{R,i,e,j} - t_{R,i,c,j})^2 \quad (17)$$

where  $j$  is the serial number of the experiments being employed in the regression, and  $n$  the total number of the experiment data being used.

The usual mathematic method is that Eq. (17) is taken a partial differential of  $k_{w,i}^0$  or  $s_i$ , to make the values of their derivatives zero, where the values of  $k_{w,i}^0$  and  $s_i$  are the desired answers, respectively. But for our cases it is very difficult to get the answers with this method. Thus we adopt a numerical value method in this paper. The numerical values of  $k_{w,i}^0$  and  $s_i$  are sought in the certain ranges ( $k_{w,i}^0$ : 1–1000 and  $s_i$ : 0.1–10) with the iterative method through computer aid. The search routine is carried out by these steps.

- (1) Insert the given initial of the minimum values of  $k_{w,i}^0$  and  $s_i$  in their corresponding ranges into Eq. (6) and acquire the value of the  $Q_{i,R}$  with Eq. (17).
- (2) Keep  $k_{w,i}^0$  constant and change  $s_i$  with a certain step length, sign the  $k_{w,i}^0$  and  $s_i$  to make the value of the  $Q_{i,R}$  minimum.
- (3) Change  $k_{w,i}^0$  with a certain step length and repeat (1) and (2) steps until having searched all values of  $k_{w,i}^0$  and  $s_i$  in their ranges, and find their appropriate values which make the  $Q_{i,R}$  value minimum.

This is a kind of basic search method. Generally speaking, in definition ranges, the larger the domains of the variances,  $k_{w,i}^0$  and  $s_i$ , and the shorter the search steps, then the higher the regression precision. However, this increases the calculation complication, and the search time arises markedly.

This shortcoming can be overcome by adopting the regional refinement method [44]. Namely, to the two parameters  $k_{w,i}^0$  and  $s_i$ , at first longer step length is adopted and rougher regression value of the parameters is obtained. Near the rougher regression value in a shorter domain of the parameters are chosen, again more precision regression values are found with relatively shorter computer time. By repeatedly shortening the domains of the two parameters and the

step length the optimum can be found at last. The regression astringency of this method is ensured by two ways.

- (1) The variety values between the two regression values got in two consecutive searching decrease gradually.
- (2) The parameter  $Q_{i,R}$  is smaller than an appropriate minimum value. In this paper,  $0.001 \times \sum_{j=1}^n t_{R,i,e,j}/n$  is as the appropriate minimum value.

If these conditions reach the estimated coefficients,  $k_{w,i}^0$  and  $s_i$ , will make  $Q_{i,R}$  minimum. This method obviously reduces the calculation complication and improves the calculation efficiency.

After the coefficients,  $k_{w,i}^0$  and  $s_i$ , have been identified, the band spread parameters,  $a_i$  and  $b_i$ , are ergodically searched with the same method mentioned above in reasonable domains (both are in  $1 \times 10^{-5}$  to 1.0). Band width recursion equation, Eqs. (14) and (16), is used in the regression process. Similar to Eq. (17) and the method of obtaining  $k_{w,i}^0$  and  $s_i$ , the band spread parameters,  $a_i$  and  $b_i$  can be obtained by making  $Q_{i,w}$  minimum:

$$Q_{i,w} = \sum_{j=1}^n (w_{1/2,t,e,j} - w_{1/2,t,c,j})^2 \quad (18)$$

where  $w_{1/2,t,i,e,j}$  and  $w_{1/2,t,i,c,j}$  are calculated and experimental half-band width time unit of the solute  $i$ .  $w_{1/2,t,c,j}$  can be got with Eqs. (14) and (16). The program frame with C++ computer language regressing the parameters,  $k_{w,i}^0$ ,  $s_i$ ,  $a_i$  and  $b_i$  is shown in Fig. 2. Fig. 3 shows the program frame of the calculation progress for the prediction of the solute retention time and half-band width.

#### 4. Experimental

An Agilent 1100 liquid chromatograph equipped with a UV detector, operated at 254 nm, manual injection, a thermostatted column compartment, and a Series G2170AA LC ChemStation workstation (Hewlett-Packard, Palo Alto, CA, USA) was used to acquire the elution data. A stainless steel column A, 50 mm  $\times$  4.6 mm i.d., packed with Silasorb C18, 5  $\mu$ m ( $t_0 = 0.506$  min) and another stainless steel cartridge column B, 150 mm  $\times$  4.6 mm i.d., packed with Silasorb C18, 5  $\mu$ m ( $t_0 = 1.400$  min) (Waters Assoc.) were used. The constant flow rate of the mobile phase was kept at 1 mL min<sup>-1</sup> and the temperature at 20 °C in all experiments.

Methanol was used as the strong eluent solvent in mobile phases with HPLC grade and obtained from Baker (Deventer, The Netherlands). The sample compounds used in this study were benzene, toluene, nitrobenzene, 2-nitrotoluene, 3-nitrotoluene, 4-nitrotoluene, phenylethanol and phenylpropanol. Sodium nitrite was used as the void marker. Water was doubly distilled and deionized in glass. Mobile phases were prepared directly in the Agilent 1100 instrument from the components continuously stripped by a stream of helium. 10  $\mu$ L sample volumes were injected in each experiment.

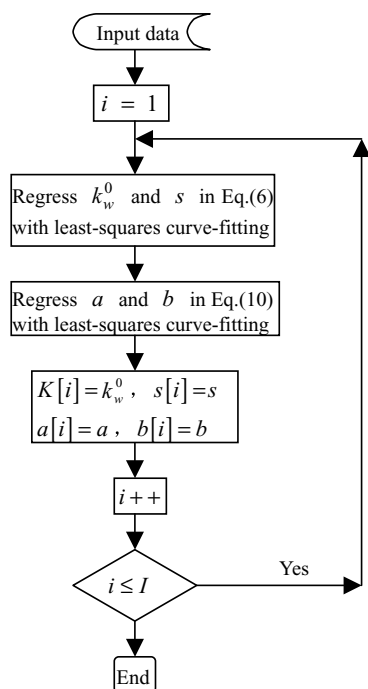


Fig. 2. The computer program frame on the regression progress of band migration and spreading parameters  $k_w^0$ ,  $s$ ,  $a$  and  $b$  with C++ language. Where  $i$  is the solute serial number;  $I$  is the solute total number;  $k[i]$ ,  $s[i]$ ,  $a[i]$  and  $b[i]$  are the arrays storing the regression values of  $k_w^0$ ,  $s$ ,  $a$  and  $b$  of the  $i$ th solute.

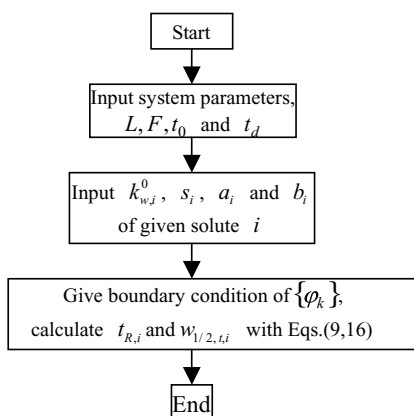


Fig. 3. Calculation progress of the solute retention time and band width in given elution mode with the computer aid.

The columns were first equilibrated with the initial concentration mobile phase before the beginning of each run. A 5-min flush time was used by 100% pure solvent after the end of each experiment to clean the column.

## 5. Results and discussion

### 5.1. Retention prediction

The data involved three species of solute series in two column systems under isocratic and gradient used to deter-

mine the regressors and to predict retention and band width. LSS model and plate theory are cited to predict the behaviours of solute zones based on same data for comparing with the model of this paper. The mean-root-square error ( $\sigma$ ) is adopted to indicate the accuracy of the prediction [45]:

$$\sigma = \sqrt{\frac{\sum_{i=1}^n [y_{c,i} - y_{e,i}]^2}{n - p}} \quad (19)$$

where  $y_{c,i}$  is the calculated value of the  $i$ th experiment through corresponding equations,  $y_{e,i}$  the experimental value of the  $i$ th experiment,  $n$  the experimental times, and  $p$  the number of fitted parameters.

For linear gradient elution HPLC, the concentration of the strong elution in a two-component mobile phase,  $\varphi$ , can be expressed as a linear gradient function:

$$\varphi = \varphi_0 + Bt \quad (20)$$

where  $\varphi_0$  is the initial concentration of the strong solvent at the start of the gradient,  $B = (\varphi_g - \varphi_0)/t_g$  the slope of the gradient controlled by the gradient time,  $t_g$ , necessary to achieve the final concentration,  $\varphi_g$ . Through the method described above, the continuous concentration function, Eq. (20), can be changed into corresponding concentration sequence  $\{\varphi_k\}$ , which is used in recursion equations to predict the retention and band width.

The retention equation of gradient elution in literature [46,47] is:

$$t_R = \frac{1}{sB} \log \left[ 2.31sBt_0 \frac{K_w^0}{10^{s\varphi_0}} + 1 \right] + t_0 + t_d \quad (21)$$

where the meanings of  $K_w^0$  and  $s$  are same as in Eq. (6). Eq. (21) is also based on Eq. (6) in linear gradient function determined by Eq. (20), which is the sum of an integral of the solute migration, the void time and the dwell time. Compared with Eq. (21), the deduction of Eq. (9) is just the combination of Eqs. (4)–(6), and expressed in the repeated addition form. Thus Eqs. (9) and (21) are identical when  $\Delta T_k$  tends to zero, and they have same precision and accuracy in predicting gradient retentions if  $\Delta T_k$  is small enough.

### 5.2. Band width prediction

A very important assumption that the uniform translation velocity ( $v$ ) and total effective diffusion coefficient ( $D$ ) of solute zones are constant in whole separation process was introduced to keep the tenability of plate theory. However, the parameters  $v$  and  $D$  are variable along with the transformation of space–time due to the variable composition of the mobile phase in gradient elution chromatography. It means that the concept of plate height is invalid in this case, such as gradient elution. In addition, even if in isocratic-elution the assumption is correct due to a constant of the plate height for given solutes, there are different plate heights for different solutes.

In column separation processes the solvent strength affects not only on the solute migration but also on the band broadening through that the retention factor affects migration velocity and diffusion coefficient [48]. One could reach the aim of optimal resolution in shorter separation time through obtaining an optimal gradient profile. Unfortunately, the theory of gradient elution chromatography has been developed to such an extent that relatively precise calculation of the retention data is achieved, but the precise calculation of the band width is not yet to be achieved, and the principle of the optimal gradient profile could not be found for the given separation system and solute couple due to the failure in precisely predicting band widths [7,14,46]. The root of the phenomenon lies in that separation scientists irrelevantly adopt plate theory to predict band width under gradient elution, for there is not at all a series of plates with the same plate height in gradient elution processes. Fig. 4 shows distinctly the effect of the concentration of the stronger solvent on diffusion coefficients under isocratic elution. The diffusion coefficients increase with the addition of the organic solvent concentration, and the increase degree changes with different solutes, which means that the local diffusion coefficients are changing according to the local concentration of the mobile phase in gradient elution processes. The different solutes have also different diffusion coefficients in the same concentration of the mobile phase. Analysts commonly calculate band widths through the number of theoretical plate with the assumption that the number of theoretical plates is independent of the mobile phase composition throughout the separation progress, but Fig. 4 indicates that the assumption is not the truth in gradient elution processes. In fact, the number of theoretical plate depends not only on the column-self, but also on the solute, concentration and composing of the mobile phase. It implies that it is not appropriate to predict half-band width with the average theoretical plates under gradient elution.

Virtually, separation scientists have known that three phenomena lead to solute band spreading under gradient elu-

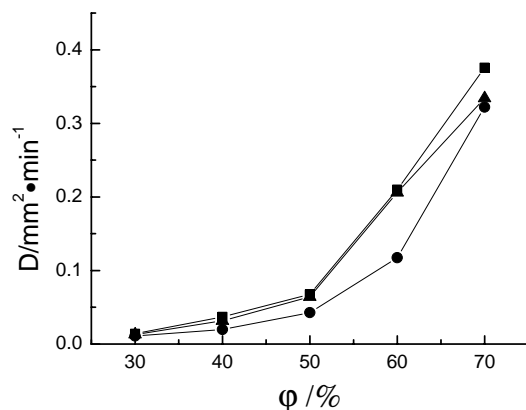


Fig. 4. Dependence of the diffusion coefficient in the isocratic elution on the mobile phase composition. The  $D$  values were calculated with Eq. (13) through experimental  $t_{R,i,e,j}$  and  $w_{1/2,t,i,e,j}$  on 50 mm column (■) 2-nitrotoluene; (●) 3-nitrotoluene; (▲) 4-nitrotoluene.

tion [13]: (a) broadening of the solute band as in isocratic elution; (b) solute band compression caused by a steady decrease in the capacity factor; (c) an addition compression of the band resulting from the fact that the front of band moves with a lower eluting strength than the end of the band. However, those ideas could not be satisfactorily applied into the practical calculations of band widths [7,8,13,14]. The phenomena (a) and (b) mean that the local diffusion coefficient  $D_{i,j,k}$  must be introduced and the phenomena (b) and (c) require that we must divide the space that solute occupies into enough many cells. Of course, Lagrangian description, the continuum axiom and local equilibrium assumption also require us to describe the evolution of solute bands in a discrete space and time format. In Eq. (2), we can consider the three phenomena leading to band spreading in a same equation. The first term on the right-hand side of Eq. (2) is for the phenomena (a) and (b) with local diffusion coefficient  $D_{i,j,k}$ . The second term on the right-hand side of Eq. (2) is for the phenomena (c) by considering the overlapping and stretching between adjacent cells. The contribution of the overlapping and stretching between adjacent cells to band widths could be neglected with high column efficiency or in linear chromatography.

For comparing with band width recursion equation, Eq. (16), the literature band-width equation [14] is cited as:

$$w = 4t_0 \frac{1 + k'_f}{\sqrt{N}} \quad (22)$$

where  $w = 4\sigma$ , and  $N$  the number of theoretical plates, which obtained from the average value from several runs. For comparing with Eq. (16) conveniently, Eq. (22) is transformed into the expression of half-band width:

$$w_{1/2,t} = \frac{\sqrt{5.55}t_0(1 + k'_f)}{\sqrt{N}} \quad (23)$$

In fact, Eq. (23) just comes from the definition formula of the number of theoretical plates. The average value adopted for the parameter  $N$  in Eq. (23) undoubtedly brings on big errors in the band width predictions, especially, in different gradient elution profiles, since the diffusion coefficient of solute zones depends on the species of solutes and the composition of mobile phases. In the processes of gradient elution, the local concentration of the mobile phase ( $\varphi_k$ ) around solute zones changes as the time and the space change, and the solute local diffusion coefficients,  $D_{i,k}$ , in Eq. (14) and solute local migration velocity,  $\bar{v}_{i,k}$ , in Eqs. (6) and (12) depend on the change of  $\varphi_k$ . Therefore accurate band-width predictions should adopt the accumulation manner of the solute local diffusion coefficients to local migration velocity and migration time of the solute. At this time, the concept of traditional theoretical plates has lost its intrinsic meaning in gradient elution. It just is the reason that Giddings inducted the local theoretical plate [1]. However, he and others did not follow it far.

The band width recursion equations, Eqs. (2) and (16), were presented by using the laws, Lagrangian description



and the continuum axiom in mechanics of continua, and the local equilibrium assumption in non-equilibrium thermodynamics. Then the chromatographic processes of solute zones were discretized by space–time cells, and the contributions of individual space–time cells to the band width were piled up in whole chromatographic processes. The relationship, Eq. (14) between the local diffusion coefficient,  $D_{i,k}$ , and the local capacity factor,  $k'_{i,k}$ , were set up with Eqs. (10)–(12), then the relationship between  $D_{i,k}$  and local concentration of the mobile phase,  $\varphi_k$ , of the solute zone was acquired through Eqs. (6) and (14). Therefore, Eqs. (2), (16) and (22) are different on both their theoretical bases and deduction processes. Eq. (16), due to taking into account the essential character that the local diffusion coefficient time-varies with local concentration of the mobile phase, should more accurately reflect the evolution of the solute band width.

Table 1 shows that the mean-root-square errors of predicted half-band widths with Eq. (16) under isocratic elution with 50 mm column ( $\sigma_m(\text{I}) = 0.0103$  or  $\sigma_m(\text{II}) = 0.0111$ ) were remarkably smaller than one's using Eq. (23) ( $\sigma_m(\text{III}) = 0.0410$ ), and there are no evident errors between adopting two data of  $w_{1/2,t,e}$ , with both 40 and 70%, and with both 40 and 60% methanol concentrations. The factors affecting the broadening of the chromatographic zones are very complicated, so it is considered acceptable that the relative errors between  $w_{1/2,t,c}$  and  $w_{1/2,t,e}$  are lower than  $\pm 10\%$  [44]. In Table 1, the domain of the relative errors of  $w_{1/2,t,c}$

in the column I using Eq. (16) is  $-6.8$  to  $10.5\%$ , which is the best among the three methods and almost within the domain of  $\pm 10\%$ . The method using Eq. (23) with the number of the theory plate for the  $w_{1/2,t,c}$  in the column 3 is the worst among the three methods, whose relative error reaches  $22.5\%$ , and it already loses prediction meanings. It is always the worst for the prediction of 3-nitrotoluene with the literature method (the column III in Table 1) for isocratic elution of different methanol concentrations. The reason is that the column efficiency or the number of theory plate is different for different solutes, which consequentially induces the considerable prediction error for some solutes if the number of theoretical plates is adopted to predict  $w_{1/2,t}$  for different solutes.

In Table 2, the band width recursion equation, Eq. (16), was applied to predict half-band width under gradient elution on the 50 mm column with  $N = 3000$ . The range of the relative errors with Eqs. (16) and (23) are in  $-5.26$  to  $9.41\%$  (lower than  $\pm 10\%$ ) and  $-55.7$  to  $27.5\%$  (obviously higher than  $\pm 27\%$ ), respectively. And the mean-root-square error for all solutes with Eqs. (16) and (23) in gradient elution are  $0.00502$  and  $0.0475$ , respectively. The mean-root-square error with the literature equation is 9.5 times the magnitude of one with the band width recursion equation. It is clear that the prediction effect of half-band width using the literature method under gradient elution is not only worse than one with the band width recursion, but also worse than the effect of itself used under isocratic elution (Table 1). The above

Table 1  
Comparison of the experimental and predicted half-band widths with different methods in isocratic elution with 50 mm column

Compound	Methanol concentration (%)	$w_{1/2,t,e}$ (min)	$w_{1/2,t,c}$ (min) <sup>a</sup>			Relative error (%) <sup>b</sup>		
			I	II	III	I	II	III
2-Nitrotoluene	40	0.5267	0.5277	0.5267	0.5652	0.19	0.00	7.30
3-Nitrotoluene		0.4963	0.4972	0.4963	0.6035	0.18	0.00	21.60
4-Nitrotoluene		0.5680	0.5673	0.5680	0.5669	-0.12	0.00	-0.19
2-Nitrotoluene	50	0.2252	0.2488	0.2488	0.2390	10.48	10.48	6.13
3-Nitrotoluene		0.2280	0.2407	0.2329	0.2792	5.57	2.15	22.48
4-Nitrotoluene		0.2543	0.2651	0.2720	0.2626	4.24	6.96	3.26
2-Nitrotoluene	60	0.1283	0.1274	0.1282	0.1183	-0.70	-0.08	-7.82
3-Nitrotoluene		0.1181	0.1295	0.1176	0.1357	9.65	-0.42	14.89
4-Nitrotoluene		0.1438	0.1340	0.1437	0.1281	-6.82	-0.07	-10.92
2-Nitrotoluene	70	0.0755	0.0755	0.0770	0.0646	0.00	1.99	-14.43
3-Nitrotoluene		0.0825	0.0825	0.0679	0.0721	0.00	-17.70	-12.55
4-Nitrotoluene		0.0781	0.0781	0.0895	0.0687	0.00	14.60	-12.01
2-Nitrotoluene	$\sigma^c$		0.0167	0.0167	0.0308			
3-Nitrotoluene			0.0121	0.0109	0.0852			
4-Nitrotoluene			0.0103	0.0148	0.0142			
$\sigma_m^d$			0.0103	0.0111	0.0410			

<sup>a</sup> The I and II columns indicate the predicted half-band widths using Eq. (16), adopting regression parameters  $a_i$  and  $b_i$  through the experimental data of  $w_{1/2,t,i}$ ,  $w_{1/2,t,e}$ , with both 40 and 70%, and with both 40 and 60% methanol concentrations, respectively. The III column indicates the predicted half-band widths using Eq. (23) and the predicted  $t_{R,i}$  in Eq. (21) through the experimental data with both 40 and 70% methanol concentrations. The number of theoretical plates,  $N = 3000$ , is the average value for the all solutes and all elution conditions listed in the table.

<sup>b</sup> The relative error of the same solute between the experimental and predicted half-band widths. It (including below two labels) has the same meaning in Tables 2 and 3.

<sup>c</sup> The mean-root-square error for the same solute under different methanol concentrations obtained through Eq. (19).

<sup>d</sup> The mean-root-square errors for the same prediction way and all solutes under different methanol concentrations obtained through Eq. (19).

Table 2  
Comparison of the predicted and experimental half-band width with different methods under gradient elutions with 50 mm column

Compound	Gradient (min)	$w_{1/2,t,e}$ (min)	$w_{1/2,t,c}$ (min) <sup>a</sup>		Relative error (%)	
			I	II	I	II
Benzene	8	0.0968	0.0971	0.1008	0.31	4.13
Toluene		0.0951	0.0901	0.1193	-5.26	25.45
Nitrobenzene		0.1095	0.1198	0.0593	9.41	-45.84
Benzene	10	0.1093	0.1093	0.1091	0.00	-0.18
Toluene		0.1032	0.1032	0.1316	0.00	27.52
Nitrobenzene		0.1277	0.1277	0.0613	0.00	-52.00
Benzene	15	0.1328	0.1361	0.1244	2.48	-6.33
Toluene		0.1313	0.1318	0.1552	0.38	18.20
Nitrobenzene		0.1300	0.1405	0.0643	8.08	-50.54
Benzene	20	0.1569	0.1569	0.1350	0.00	-13.96
Toluene		0.1605	0.1605	0.1779	0.00	10.84
Nitrobenzene		0.1493	0.1493	0.0661	0.00	-55.73
Benzene	$\sigma$		0.00234	0.03234		
Toluene			0.00355	0.03366		
Nitrobenzene			0.01039	0.09531		
$\sigma_m$			0.00502	0.0475		

<sup>a</sup> The I column indicates predicted half-band width under gradient elution using Eq. (16), adopting regression parameters  $a_i$  and  $b_i$  through the experimental data,  $w_{1/2,t,exp}$ , with 10, 15 and 20 min linear gradient elution times and 40–100% methanol concentrations. And the II column indicates the predicted half-band width using Eq. (23) with the same calculation way as Table 1, and where  $N = 4000$ .

discussion explains that the considerable errors will arise as long as the concept of theoretical plates is adopted to predict band widths under gradient elution, since the local migration velocity, local diffusion coefficient, and local capacity factor of the volume elements (cells) of solute zones are time-varying with the local concentration of mobile phase.

Table 3 shows comparison results of predicted half-band width with Eqs. (16) and (23) under gradient elution on 150 mm-column with  $N = 5500$ . The relative error ranges using with Eqs. (16) and (23) are in -0.02 to 2.38% (lower than  $\pm 3\%$ ) and -25.9 to 15.2% (obviously higher than  $\pm 15\%$ ), respectively. And the total mean-root-square error for different solutes and gradient elution profiles with Eqs. (16) and (23) are 0.0009 and 0.0165, respectively. The

mean-root-square error with the literature equation is 18.3 times the magnitude of one with the band width recursion equation. In addition, the simulated  $w_{1/2,t}$  with Eq. (16) versus the single experimental  $w_{1/2,t}$  for the three series (13 times) of the experiments under linear gradient elution on 50 mm column were shows in Fig. 5. The agreement between the predicted values and the experimental  $w_{1/2,t}$  was quite good. The repeated experiments were not carried out in this paper, so there are remarkable non-systematic errors under a certain degree.

Under gradient elution the separation system is always in the state of non-equilibrium thermodynamics. The concentration of the mobile phase ( $\varphi_k$ ) are changing according to the separation time, solute local diffusion coefficients ( $D_{i,k}$ )

Table 3  
Comparison of the predicted and experimental half-band width with different methods in gradient elutions with 150 mm column

Compound	Gradient (min)	$w_{1/2,t,e}$ (min)	$w_{1/2,t,c}$ (min) <sup>a</sup>		Relative error (%)	
			I	II	I	II
Phenylethanol	5	0.0614	0.0614	0.0571	0.06	-6.93
Phenylpropanol		0.0575	0.0575	0.0663	0.02	15.25
Phenylethanol	10	0.0803	0.0803	0.0684	0.02	-14.81
Phenylpropanol		0.0757	0.0775	0.0847	2.38	11.84
Phenylethanol	20	0.1044	0.1044	0.0773	0.01	-25.93
Phenylpropanol		0.1079	0.1079	0.1015	-0.02	-5.97
Phenylethanol	$\sigma$		0.00005	0.02990		
Phenylpropanol			0.00180	0.01410		
$\sigma_m$			0.00090	0.01650		

<sup>a</sup> The I column indicates the predicted half-band widths under gradient elution using Eq. (16), adopting regression parameters  $a_i$  and  $b_i$  through  $w_{1/2,t,e}$  with 5, 10 and 20 min linear gradient elution times and 50–100% methanol concentrations. And the II column indicates the predicted half-band widths using Eq. (23) with the same calculation way as Table 1, and where  $N = 5500$ .

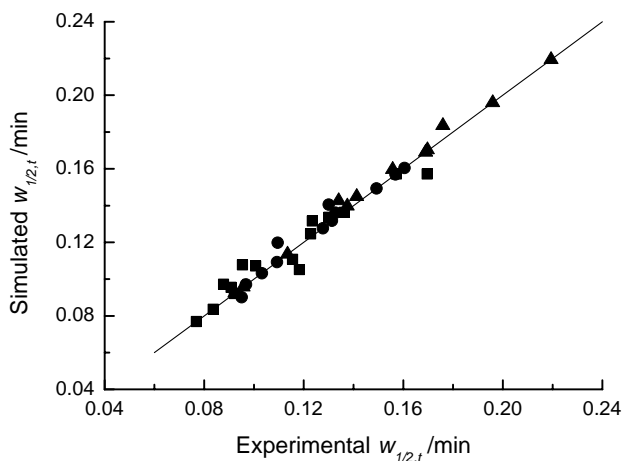


Fig. 5. The simulated  $w_{1/2,t}$  with Eq. (16) vs. the experimental  $w_{1/2,t}$  for the three series of linear gradient elution experiments on the 50 mm column ((■) 30–100% methanol concentrations in 5, 8, 10, 15, 20 min; (●) 40–100% in 8, 10, 15, 20 min; (▲) 40–80% in 5, 10, 15, 20 min).

are changing according to  $\varphi_k$ . In this paper  $D_{i,k}$  was related to  $\varphi_k$  in Eq. (14), so  $w_{1/2,t}$  was described as the iterative addition arising from each discrete time unit contribution to band broadening in Eq. (16). Therefore, Eq. (16) describes the evolution process of the band broadening more accurately under gradient elution. The prediction under gradient elution was worse than the prediction in isocratic elution with Eq. (23), since an average value of the number of theoretical plates for different solutes and gradient elution profiles, which directly leads to considerable errors.

Recursion of separation states in space- and time-dependent fields is a universal method in dealing with the evolution of solute zones in column separation processes. A basic application of recursion equations is to accurately calculate retention times and band widths under given space- and time-dependent fields (e.g. pre-set gradient profiles). Recursion equations certainly enlarge the theories of band spreading from constant fields (e.g. isocratic elution chromatography) to space- and time-dependent fields (e.g. gradient elution chromatography). However, a more important application of the recursion equations is in finding an optimal thermodynamic separation path in the ergodic phase-space (a phase plane constructed by two vertically coordinates of the operation parameter and time) through using non-equilibrium thermodynamic separation theory [2,20,22–27], multi-stage decision and optimal control methods. Recursion equations are essential in the optimal control of separation processes [31,32].

## 6. Conclusion

(1) The evolution of solute zones in space- and time-dependent fields can be described by the iterative addition of local density of solute zones with the mesoscopic approach, which involved Lagrangian descrip-

tion, the continuity theory and the local equilibrium assumption.

- (2) The recursion equations were proposed to predict the evolution (migration and spreading) of solute zones in RP-HPLC through directly relating the local retention factor and the local diffusion coefficient to the local mobile phase concentration. Actually, band width recursion equation is the accumulation of local diffusion coefficients of solute zones to a series of discrete-time slices.
- (3) The comparison results of the recursion equations and literature equations dealing with the same experimental data of zone migration and spreading in RP-HPLC show that the recursion equations can more accurately predict band width under gradient elution. Though the concept of theory plate is appropriate to indicate column efficiency, it fails to predict band width under gradient elution.

## 7. Nomenclature

$a_i, b_i$	experimental constants of the component $i$ in Eq. (10)
$B$	the slope of linear gradient function
$c_{i,j,k}$	local molar concentration of the component $i$ in the volume element $j$ at the time $t_k$ . The subscript marker, $i, j, k$ , indicates local parameter of the component $i$ in the volume element $j$ at the time $t_k$
$D_{i,j,k}$	local diffusion coefficient
$E_{i,j,k}$	local electrical field strength
$F$	volume flow rate of mobile phase
$i$	the serial number of solute components
$j$	the serial number of volume elements or the experiments employed in the regression
$k$	the serial number of the time $t_k$
$k'_f$	the instantaneous capacity factor when the peak maximum of solute zone is just passing the end of the column
$k'_{i,j,k}$	local capacity factor
$k'_{i,k}$	predigest local capacity factor
$\{k'_{i,k}\}$	the sequence of local capacity factor
$k_{w,i}^0, s_i$	experimental parameters of the component $i$ in LSS model
$K_{i,j,k}$	local thermodynamic distribution constant
$L$	column length
$m_{i,j,k+1}$	volume element width along column axes of the cell $j$ of solute $i$ at the time $t_{k+1}$
$n$	the experimental times in Eq. (17)
$N$	the number of theoretical plates

$p$	the number of fitted parameters	$\varphi_0$	the initial concentration of the strong solvent at the start of the gradient
$Q_{i,R}$	the sum of squares of absolute error between calculated and experimental retention time of the component $i$	$\varphi_{i,j,k}$	local strong eluent concentration of mobile phase
$Q_{i,w}$	the sum of squares of absolute error between calculated and experimental half-band width of the component $i$	$\varphi_{i,k}$	predigest local strong eluent concentration of mobile phase
$t_0$	the column dead time	$\{\varphi_k\}$	the strong eluent concentration sequence at the pump head
$t_d$	gradient dwell time	$\lambda_{i,k}$	the stretch ratio of volume elements at time $t_k$
$t_g$	the gradient time	$\mu_{i,j,k}$	local chemical potential
$t_k$	the $k$ point at time axis	$\rho_{i,j,k}, \rho_{i+1,j,k}$	local solute densities of the two components, $i$ and $i+1$
$t_{R,i}$	retention time of solute $i$	$\rho_{i,j,k=0}, \rho_{i+1,j,k=0}$	local solute densities at initial time $t_{k=0}$
$t_{R,i,c,j}$	the calculated retention time of solute $i$ of the $j$ th data	$\rho_i(x, t_0), \rho_{i+1}(x, t_0)$	macro density distributions at initial time $t_0$
$t_{R,i,e,j}$	the calculated retention time of solute $i$ of the $j$ th data	$\sigma$	standard deviation of solute zone distribution
$\Delta\tau_{i,j}$	It needs time that volume element $j$ passes the detector ( $X_{i,K} = L$ )	$\sigma_d$	the standard deviation of solute band arose from gradient dwell time $t_d$
$\Delta t_{i,k}$	the $k$ th time interval of solute $i$	$\sigma_{i,k}, \sigma_{i,k+1}$	the standard deviation of the solute band $i$ at the times $t_{i,k}$ and $t_{i,k+1}$
$\Delta t_k$	the $k$ th given constant time interval		
$u_{j,k}$	space- and time-dependent field acting on $j$ th volume element $j$ at the time $t_k$		
$\bar{v}_{i,j,k}, \bar{v}_{i+1,j,k}$	local migration velocity of the components, $i$ and $i+1$ , respectively		
$\bar{v}_{i,k}$	predigest local migration velocity of the component $i$		
$V_0$	injected solute column volume		
$w_{1/2}$	half-band width, band-width half band width at height		
$w_{1/2,l}$	half-band width in length units		
$w_{1/2,t}$	half-band width in time units		
$w_{1/2,t,c,j}$	experimental half-band width time unit of the solute $i$ of the $j$ th data		
$w_{1/2,t,i,e,j}$	experimental half-band width time unit of the solute $i$ of the $j$ th data		
$x$	the direction of separation paths		
$X_{i,j,k}, X_{i,j,k+1}$	the positions of the volume element $j$ in stationary phase at the time $t_{i,k}$ and $t_{i,k+1}$ , respectively		
$X_{i,K}$	the position at the column terminal of solute $i$ at the end of separation process		
$X_{i,0}$	the position at the column inlet of solute $i$ at the run beginning		
$y_{c,i}$	the calculated value of the $i$ th experiment through corresponding equations		
$y_{e,i}$	the experimental value of the $i$ th experiment		
<b>Greek letters</b>			
$\delta_{i,j,k=0}$	the length of the volume element $j$ on the $x$ axis along separation path at initial time $t_{k=0}$		

### Acknowledgements

This work was financially supported by the National Natural Science Foundation of China (Approval Nos. 20299030, 20175015 and 29775017). The authors gratefully acknowledge Huabing Gao and Xiaowei Ding for their assistance of computer program.

### References

- [1] J.C. Giddings, Unified Separation Science, Wiley/Interscience, New York, 1991, p. 10.
- [2] H. Liang, B.-Ch. Lin, J. Chromatogr. A 828 (1998) 3.
- [3] W.Q. Sun, G.R. Yu, W.H. Yan, J. High Resolut. Chromatogr. 13 (1990) 173.
- [4] G. Vivo-Truyols, J.R. Torres-Lapasio, M.C. Garcya-Alvarez-Coque, J. Chromatogr. A 876 (2000) 17.
- [5] S.G. Lisseter, Lab. Microcomput. 9 (4) (1990) 109.
- [6] P.F. Vanbel, J. Pharm. Biomed. Anal. 21 (1999) 603.
- [7] L.R. Snyder, J.W. Dolan, J.R. Gant, J. Chromatogr. 165 (1979) 3.
- [8] L.R. Snyder, M.A. Stadalius, in: Cs. Horváth (Ed.), High Performance Liquid Chromatography—Advances and Perspectives, vol. 4, Academic Press, New York, 1986.
- [9] P.J. Schoenmakers, H.A.H. Billiet, R. Tijssen, L. de Galan, J. Chromatogr. 149 (1978) 519.
- [10] P.J. Schoenmakers, H.A.H. Billiet, L. de Galan, J. Chromatogr. 282 (1983) 107.
- [11] X.-D. Geng, F.E. Regnier, J. Chromatogr. 296 (1984) 15.
- [12] X.-D. Geng, F.E. Regnier, Chromatographia 38 (1994) 158.
- [13] P. Jandera, J. Churacek, Gradient Elution in Column Liquid Chromatography, Elsevier, New York, 1985.
- [14] P. Jandera, J. Chromatogr. A 845 (1999) 133.
- [15] A.J.P. Martin, R.L.M. Synge, J. Biochem. 35 (1941) 1358.



- [16] J.J. van Deemter, F.J. Zuiderweg, A. Klinkenberg, *Chem. Eng. Sci.* 5 (1956) 271.
- [17] L.C. Craig, *J. Biol. Chem.* 155 (1944) 519.
- [18] C. Horvath, H.J. Lin, *J. Chromatogr.* 149 (1978) 43.
- [19] H. Poppe, J. Paanakker, M. Bronckhorst, *J. Chromatogr.* 204 (1981) 77.
- [20] H. Liang, W.-H. Tan, *Acta Chim. Sinica* 58 (2000) 935 (in Chinese).
- [21] S.C. Hunter, *Mechanics of Continuous Media*, second ed., Ellis Horwood, New York, 1983.
- [22] H. Liang, Ph.D. dissertation, Beijing Institute of Technology, Beijing, 1995 (in Chinese).
- [23] H. Liang, Zh.-G. Wang, B.-Ch. Lin, Ch.-G. Xu, R.-N. Fu, *J. Chromatogr. A* 763 (1997) 237.
- [24] H. Liang, B.-C. Lin, Presented at the 22nd International Symposium on High-Performance Liquid Phase Separations and Related Techniques, St. Louis, MO, 2–8 May 1998, Book of Abstracts, 1998, p. 167.
- [25] H. Liang, B.-Ch. Lin, *J. Chromatogr. A* 841 (1999) 133.
- [26] Y.-P. Li, L. Yu, Y.-B. Xie, H. Liang, *Acta Chim. Sinica* 57 (1999) 281 (in Chinese).
- [27] H. Liang, Chinese Patent, Application No. 00113748.4 (in Chinese).
- [28] N. Wiener, *Cybernetics—Or Control and Communication in the Animal and the Machine*, Wiley, New York, 1948.
- [29] Istvan Gyarmati, *Non-Equilibrium Thermodynamics*, Springer-Verlag, Berlin, 1970, p. 6.
- [30] I. Prigogine, *Introduction to Thermodynamics of Irreversible Processes*, third ed., Wiley, New York, 1967.
- [31] A.E. Bryson Jr., Y.C. Ho, *Applied Optimal Control—Optimization, Estimation, and Control*, Wiley, New York, 1975.
- [32] F.L. Lewis, *Optimal Control*, Wiley, New York, 1986.
- [33] A.C. Eringen, *Mechanics of Continua*, second ed., Robert E. Krieger Pub. Co., 1980.
- [34] S.C. Hunter, *Mechanics of Continuous Media*, second ed., Ellis Horwood, New York, 1983.
- [35] P. Coveney, R. Highfield, *The Arrow of Time: A Voyage Through Science to Solve Time's Greatest Mystery*, W.H. Allen, London, 1990.
- [36] A.H. Anderson, T.C. Gibb, A.B. Littlewood, *J. Chromatogr. Sci.* 8 (1970) 640.
- [37] W.W. Yau, *Anal. Chem.* 49 (1977) 395.
- [38] R. Serra, M. Anderotta, M. Compiani, G. Zanarini, *Introduction to the Physics of Complex Systems: The Mesoscopic Approach to Fluctuations, Non Linearity and Self-Organization*, Pergamon Press, Oxford, 1986.
- [39] F. Dondi, G. Guiochon (Eds.), *Theoretical Advancement in Chromatography and Related Separation Techniques*, Kluwer Academic Publishers, Dordrecht, 1992, pp. 1–33, 173–210.
- [40] P.D. Grossman, J.C. Colburn (Eds.), *Capillary Electrophoresis: Theory and Practice*, Academic Press, San Diego, 1992.
- [41] L.R. Snyder, M.A. Buarry, *J. Liq. Chromatogr.* 10 (1978) 1789.
- [42] P.Z. Lu, Y.K. Zhang, X.M. Liang, *The High-Performance Liquid Chromatography and Its Expert System*, Liaoning Science and Technology Press, Shen Yang, 1992 (in Chinese).
- [43] M.B. Douglas, G.W. Donald, *Nonlinear Regression Analysis and Its Application*, Wiley, New York, 1988, pp. 32–133.
- [44] Z.-H. Ma, *Handbook of Modern Mathematics Application—Operational Research and Optimization Theory*, Tsinghua University Press, Peking, 1998 (in Chinese).
- [45] D. Donald, G. Thomas, *Water Res.* 32 (1998) 840.
- [46] L.R. Snyder, J.W. Dolan, *Adv. Chromatogr.* 38 (1998) 115.
- [47] N. Lundell, *J. Chromatogr.* 639 (1993) 97.
- [48] E. Katz, R. Eksteen, P. Schoenmakers, N. Miller, *Handbook of HPLC*, Marcel Dekker, New York, 1998.